Structural characterization of the circulating soluble FGF receptors reveals multiple isoforms generated by secretion and ectodomain shedding

Anne Hanneken*

The Scripps Research Institute, Department of Cell Biology, 10550 North Torrey Pines Road, La Jolla, CA 92037, USA

Abstract Soluble fibroblast growth factor receptors (FGFRs) have been identified in multiple biological fluids, including blood. Efforts to examine the biological properties of these proteins have been hampered by the incomplete chemical characterization of the receptors within the second half of the third immunoglobulin (Ig)-like domain, where alternative splicing leads to receptor variants with different ligand binding properties. Using mass spectrometry techniques, we have mapped the soluble FGFRs to the secreted receptor, FGFR1(IIIa), the two and three Ig-like domain isoforms of FGFR1(IIIc) and a carboxyl-terminal cleavage peptide from the two and three Ig-like domain isoforms of FGFR1(IIIb). The secreted FGFR is produced by the translation of an alternatively spliced transcript and the cleaved receptors are released by ectodomain shedding of the transmembrane receptors. © 2001 Federation of European Biochemical Societies. Published by Elsevier Science B.V. All rights reserved.

Key words: Fibroblast growth factor; FGF-2;
Soluble receptor; Isoform; Ectodomain shedding; Calf serum

1. Introduction

Soluble receptors are part of an expanding class of regulatory molecules that are derived from the extracellular domains of integral plasma membrane proteins (for review see [1,2]). Their ligand binding affinities are often similar to those of the cell surface receptor, suggesting that their biological role is to modulate the systemic and local action of their ligands by competing with the cell surface receptors for ligand binding. A few soluble receptors are generated by the secretion of alternatively spliced mRNA transcripts, which have been identified in cDNA libraries and/or predicted from genomic sequences [1]. However, most soluble receptors are generated by proteolytic cleavage at the cell surface by sheddases, many of which are members of the ADAMs (a disintegrin and metalloprotease) family of metalloproteases [2]. The shedding of soluble receptors provides a key mechanism for the downregulation of cell surface receptors and the release of biologically active proteins into the circulation [2–6].

We have identified soluble fibroblast growth factor receptors (FGFRs) in multiple biological fluids, as well as in the extracellular matrix of vascular endothelial cells [7–9]. One group of soluble FGFRs has a molecular mass ranging from 55 to 60 kDa and consists of the two immunoglobulin (Ig)-like domain isoforms of FGFR1. A second group has a molecular mass of 85 kDa and corresponds to the three Ig-like domain isoforms of FGFR1. It has been proposed that the soluble FGFRs function as endogenous inhibitors of the biological activities of the FGF family of proteins in vivo, both in the circulation and in the extracellular matrix [7,10]. However, until the proteins have been fully structurally characterized, the question of their biological properties remains largely speculative.

There is structural and functional diversity within the high affinity FGFR gene family [11]. There are four related FGFR gene family members and among these, FGFR1, 2, and 3 encode different isoforms that are generated by alternative splicing of mRNA transcripts [12–16]. These isoforms include receptors lacking Ig-like domain I and/or containing alternative sequences in the second half of Ig-like domain III [13,14] (Fig. 1). The latter group includes variants that consist of two alternative transmembrane forms of the high affinity FGFR (IIIb or IIIc) and a secreted form that lacks the transmembrane domain (IIIa). This structural diversity has functional relevance because the various isoforms of the transmembrane FGFRs have different affinities for the FGF family members [17,18].

To understand the functional significance of the soluble FGFRs, it is necessary to classify them according to the presence or absence of Ig-like domain I and the specific exon (IIIa, IIIb, or IIIc) encoding the second half of the Ig-like domain III. To accomplish this goal, we performed matrix-assisted laser desorption/ionization time-of-flight (MALDI-TOF) mass spectrometry (MS) and confirmed these results using nanoelectrospray MS/MS or postsource decay (PSD) on tryptic fragments of the soluble FGFRs purified from blood. Using sequence analysis programs, we mapped the second half of the third Ig-like domain within the region coded by exons IIIa, IIIb, and IIIc.

_____
*Fax: (1)-858-784 7675.
E-mail: ahanneke@scripps.edu

2. Materials and methods

2.1. Materials

Human recombinant FGF-2 was expressed in *Escherichia coli* [19] and purified using heparin-Sepharose affinity chromatography and ion-exchange chromatography as previously described [20]. Monoclonal antibodies (Mab6) to the extracellular domain of the recombinant FGFR1 [21] were raised in ascites fluid and purified over Protein G-Sepharose columns (Amersham Pharmacia Biotech, Piscataway, NJ, USA) [10].

2.2. Immunoblotting

Soluble FGFRs were identified by immunoblotting on 8% sodium dodecyl sulfate–polyacrylamide agarose gel electrophoresis (SDS–PAGE) gels. The proteins were transferred to nitrocellulose, blocked for 1 h at room temperature with 5% non-fat milk in Tris-buffered saline (TBS), 0.1% Tween 20, and then immunoblotted overnight at 4°C with 2 μg/ml of Mab6 diluted in 5% bovine serum albumin in TBS, 0.05% Tween 20. The blots were washed with TBS, 0.05% Tween 20 and incubated for 1 h at room temperature with horseradish peroxidase-conjugated goat anti-mouse antibodies (Bio-Rad) diluted 1/5000 in 5% non-fat milk in TBS, 0.1% Tween 20. The immunoblots were developed with the Super Signal reagent (Pierce, Rockford, IL, USA) according to the manufacturer's instructions.

2.3. Purification of the soluble FGFRs from calf serum

The 85 kDa and the 55–60 kDa soluble FGFRs were purified from 1 l aliquots of newborn calf serum (Omega Scientific, Tarzana, CA, USA) using 8 ml HS affinity columns (Amersham Pharmacia Biotech, Piscataway, NJ, USA) containing 10 mg recombinant FGF-2 according to standard protocols [7]. The 2 M NaCl eluates from the FGF/HS columns were concentrated using a Centriplus concentrator (Millipore, Bedford, MA, USA) and loaded on a Model 491 Prep Cell electrophoresis column (Bio-Rad, Hercules, CA, USA) containing an 8% SDS–PAGE gel and eluted according to the manufacturer's protocol. The 55–60 kDa and the 85 kDa soluble FGFR fractions were concentrated and deglycosylated using a combination of PNGase F, sialidase A, Endo-*O*-glycosidase, β(1-4)galactosidase and glucosaminidase included in the GlycoPro deglycosylation kit (ProZyme, San Leandro, CA, USA) according to the manufacturer's instructions. The deglycosylated proteins were separated on an 8% SDS–PAGE gel, stained with GELCODE blue stain reagent, destained in water and excised from the gel. For MS, the excised gel pieces were washed with 25 mM ammonium bicarbonate containing 30% acetonitrile, dried and rehydrated in ammonium bicarbonate, pH 8.0. Modified sequence grade trypsin (Promega, Madison, WI, USA) was added at a concentration of 0.1 mg/ml and incubated at 30°C overnight. The supernatant was removed and the tryptic fragments were extracted several times using 60% acetonitrile/0.01% trifluoroacetic acid (TFA) at 30°C.

2.4. MALDI-TOF MS

All MS studies were performed by the Mass Spectrometry Core Facility at The Scripps Research Institute. The masses of the digested tryptic fragments were analyzed by MALDI-TOF-reflectron using a Voyager-Elite time-of-flight mass spectrometer with delayed extraction (PerSeptive Biosystems, Inc., Framingham, MA, USA). A volume of 1 μl of digested protein was placed directly on the MALDI analysis plate, mixed with 1 μl of matrix (α-cyano-4-hydroxy-cinnamic acid) in a saturated solution of acetonitrile/water (50:50 v/v) with 0.25% (w/w) TFA and inserted into the MALDI ionization source for analysis. The samples were irradiated with a nitrogen laser (Laser Science, Inc.) operated at 337 nm. The laser beam was attenuated onto the sample target by a neutral density filter. Ions produced by laser desorption were typically energetically stabilized during a delayed extraction period of 150 ns and were then accelerated through the time-of-flight mass analyzer with a 20 kV potential. Typically, the spectra were an average of 128 laser pulses. The measurements were internally calibrated and the peaks were assigned in the linear mode with an accuracy of 1000 ppm. The monoisotopic mass was used to assign peaks with masses < 1400.0 Da and the average mass was used to assign peaks with masses > 1400.0 Da. The exact mass measurements were performed using the same MALDI instrument in the reflector mode with internal calibration of trypsin fragments (VATVSLRP, MH+ 842.5099, monoisotopic mass) and (LGEHNIDVLEGNEQFINAAK, MH+ 2211.1046, monoisotopic mass).

PSD spectra were obtained for several peptides after isolation of a precursor ion using timed-ion selection. The fragment ions were reflected onto the final detector by scanning the reflector voltage at the following ratios: 1.0, 0.9, 0.81, 0.73, 0.66, 0.59, 0.53, 0.48, 0.43, and 0.39.

2.5. Mass mapping

The observed peptide masses were mapped to the expected tryptic fragments of the FGFRs using the updated protein sequence analysis program for MS, PAWS- (June 2000; PAWS- http://www.proteometrics.com/software/paws.htm). The human amino acid sequences used for this analysis were derived from the GenBank accession numbers described in Table 1. These include the secreted receptor FGFR1(IIIa), and the extracellular domain of the two and the three Ig-like loop isoforms of the transmembrane receptors, FGFR1(IIIb) and FGFR1(IIIc).

2.6. Nanoelectrospray ionization (nanoESI)-MS/MS

The nanoESI-MS experiments are performed on an API III Perkin Elmer SCIEX triple quadrupole mass spectrometer with a Protana nanoESI source. The electrospray samples are typically introduced into the mass analyzer at a rate of ∼40 nl/min. The positive and negative ions, generated by charged droplet evaporation, enter the analyzer through an interface plate and a 100 μm orifice, while the declustering potential is maintained between 50 and 200 V to control the collisional energy of the ions entering the mass analyzer. The emitter voltage is typically maintained at 800 V. A curtain gas of ultrapure nitrogen was pumped into the interface at a rate of 0.6 l/min to aid evaporation of solvent droplets and to prevent particulate matter from entering the analyzer. The digested protein (3 μl) was mixed with 7 μl of MeOH and 0.5 μl formic acid (for fragment ion scan), 4 μl of which was loaded into a palladium-coated borosilicate glass capillary and injected into the mass spectrometer. The fragment ion scan was used to obtain the sequence information of the interesting ions.

3. Results

3.1. Identification of the secreted FGFR, FGFR1(IIIa)

The MALDI-TOF mass spectrum of the 55–60 kDa soluble FGFRs (Fig. 2) was mapped to the tryptic peptides of the secreted FGFR, FGFR1(IIIa). The observed fragments matched 53% of the total sequence of FGFR1(IIIa) and 57% of the unique sequence in the region encoded by exon IIIa (Fig. 3). Exact mass measurements of two fragments,
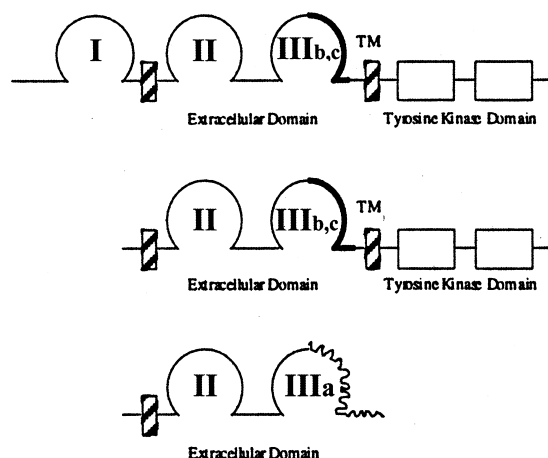

Fig. 1. Structural features of the three and two Ig-like domain isoforms of the transmembrane FGFR1 receptor (which both exist as IIIb or IIIc) and the two Ig-like domain isoform of the secreted FGFR1(IIIa) [11,13]. The divergent amino acid sequences in isoforms IIIa, b and c are indicated by bold or wavy lines.
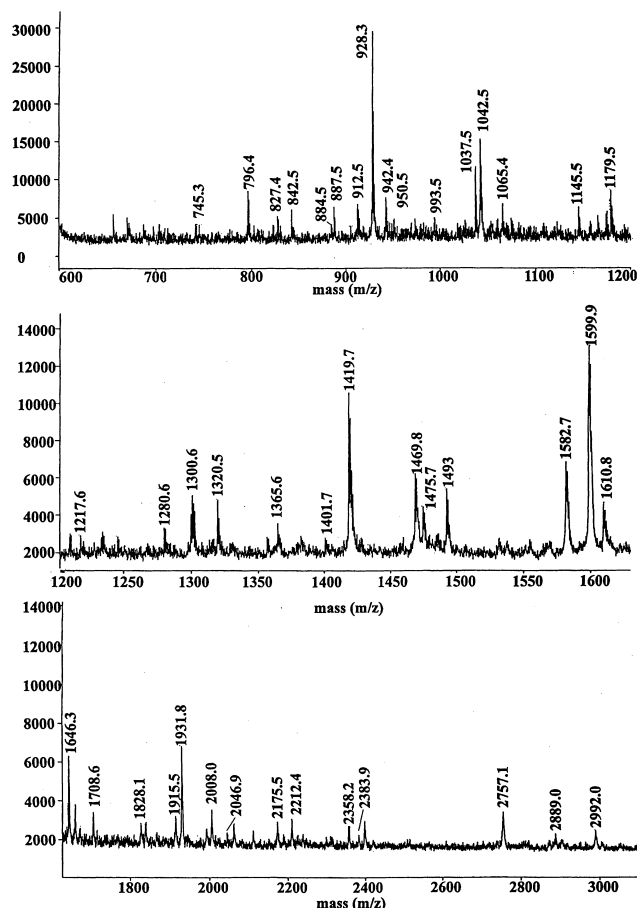
Fig. 2. MALDI-TOF mass spectrum of the tryptic digests of the 55–60 kDa soluble FGFRs derived from calf serum. The monoisotopic mass was used to assign peaks with masses < 1400.0 Da and the average mass was used to assign peaks with masses > 1400.0 Da. 81% of the major peaks in the spectrum were identified. Due to the heavily glycosylated nature of the soluble FGFRs, the unassigned peaks are attributed to incompletely deglycosylated fragment ions or ions containing other post-translational modifications.

Table 1
Amino acid sequences of the FGFR isoforms

FGFR1	Species	Reference	GenBank accession numbers
FGFR1(IIIa)-h5	Human	[13]	M34188
FGFR1(IIIc)-two Ig loop-h2	Human	[13]	M34185
FGFR1(IIIc)-three Ig loop-h1	Human	[12]	X52833
FGFR1(IIIb)	Mouse[a]	[26]	AAF05312

The amino acid sequences used for the mass mapping analyses were derived from the GenBank accession numbers indicated in this table.
[a]Because the human sequence of exon IIIb is incomplete, we used the murine sequence of exon IIIb. The murine sequence is 100% homologous to the human sequence in the corresponding regions.

on the tryptic peptide, $MH^+ = 1217.6226$, which maps to D[250–260]R in the region encoded by exon IIIa. The spectrum shown in Fig. 4 demonstrates the sequence-specific fragmentation pattern of the common b and y ions, and the less common a, b and x, z ions. The additional peaks in the spectrum consist of ions that were likely generated from other peptides that were within the timed-ion selection window used to isolate the peptide of interest. The inset shows the major ion fragments that were found in the spectrum using the nomenclature according to Biemann [22].

3.2. Identification of a cleaved two Ig-like domain isoform of FGFR1(IIIc)

The MALDI-TOF data of the 55–60 kDa soluble FGFRs were mapped to the unique sequence in the region encoded by exon IIIc. Of the three potential tryptic peptides within this region, we observed multiple fragments that matched two of the three tryptic peptides (MH^+ 1042.5, E[211–218]R+M[O]; MH^+ 1915.5, T[202–218]R and MH^+ 1931.8, T[202–218]R+M[O]) (Fig. 3). An exact mass measurement obtained on fragment MH^+ 1042.5362 Da is within 0.7 ppm of the calculated exact mass of the tryptic peptide (Table 2).

NanoESI tandem MS analyses also support the identification of soluble FGFR1(IIIc). The spectrum of the sequence-specific fragmentation pattern of the tryptic peptide, MH^+ 1042.5362 Da, is shown in Fig. 5. The inset shows the fragment ions that were found in the spectrum. The unlabeled peaks consist of internal fragments.

MH^+ 1300.6826 and MH^+ 1217.6226, are within 0.9 and 2.7 ppm of the calculated exact masses of the tryptic peptides (Table 2).

PSD-MALDI-TOF data support the identification of FGFR1(IIIa). A PSD fragmentation pattern was obtained

Peptide Mass Mapping

Exon IIIa   vimapvfvgqstgk **ETTVSGAQVPVGR LSCPRMGSFLTLQAHTLHLSR**
DLATSPRTSNR ghk vevsweqr aagmggagl

Exon IIIb   hsginssdaevltlfnvteaqsgeyvck vsnyigeanqsawltvtrpvak **ALEERPAVM*** tsplyle

Exon IIIc   **TAGVNTTDKEMEVLHLR** nvsfedageytclagnsiglshhsawltvlealeerpav*
mtsplyle

Fig. 3. Peptide mass mapping of the tryptic digests of the 55–60 kDa soluble FGFRs to exons III(a–c) of FGFR1. The peptides confirmed by peptide mass mapping are highlighted by capital letters. The small letters indicate fragment ions that were not observed. The putative carboxyl-terminal cleavage site is indicated by an asterisk.

Table 2
Exact mass measurements of the soluble FGFRs

FGFR1 residues	Observed mass	Calculated mass	Error (ppm)	Isoform specificity
E[31–39]R	1074.5194	1074.5179	1.4	IIIa,b,c
E[213–220]R+M[O]	1042.5362	1042.5355	0.7	IIIc
E[85–91]R	928.4605	928.464	3.8	IIIa,b,c
E[216–228]R	1300.6826	1300.6861	2.7	IIIa
D[250–260]R	1217.6226	1217.6237	0.9	IIIa
D[49–60]R	1345.7039	1345.6823	16	domain I
A[252–259]V	884.4568	884.4841	31	IIIb
T[64–80]R	1832.9445	1832.9694	14	IIIa,b,c
I[191–203]K	1469.8819	1469.8369	31	IIIa,b,c
W[81–86]K	745.4107	745.4361	34	IIIa,b,c

The exact mass measurements were determined by MALDI-TOF using the reflector mode with internal calibration as outlined in Section 2.

3.3. Identification of a cleaved three Ig-like domain isoform of FGFR1(IIIc)

The MALDI-TOF spectra of the 85 kDa protein sample were mapped to the sequence in the extracellular domain of the three Ig-like domain form of FGFR1(IIIc). 36% of the extracellular domain of the three Ig-like domain form of FGFR1 was matched. Two fragments were identified which matched the unique peptide within the first Ig-like domain of FGFR1, tryptic fragments (L[37–48]R) and an oxidized form of the same fragment (L[37–48]R+16, W[O]). Another two fragments were identified which span two of the three peptides from the unique carboxyl-terminal amino acid sequence in FGFR1(IIIc), tryptic peptides T[293–309]R and an oxidized form of the same fragment, T[293–309]R+16, M[O] (Fig. 3). These ionizable fragments were also detected in the MALDI-TOF analysis of the 55–60 kDa soluble FGFR samples, suggesting that calf serum contains both a two and a three Ig-like domain isoform of FGFR(IIIc) which are proteolytically cleaved from the transmembrane receptor.

3.4. Identification of a carboxyl-terminal peptide from a cleaved two and three Ig-like domain isoform of FGFR1(IIIb)

The MALDI-TOF data from both the 55 kDa and the 85 kDa soluble FGFR samples were mapped to the unique sequence in the region coded by exon IIIb. One of three potential tryptic peptides from this region was matched. This peptide (MH[+] 884.4568 = A[252–259]V) corresponds to a carboxyl-terminal peptide containing a valine–methionine cleavage site near the transmembrane domain of FGFR1(IIIb) (Fig. 3). This fragment maps to the tryptic peptide (ALEERPAV)[1] which is just eight amino acids upstream from the transmembrane domain of FGFR1. Although we were unable to obtain MS/MS or PSD data on this peptide, an exact mass measurement of this fragment (MH[+] 884.4568) was within 31 ppm of the calculated exact mass (Table 2). This assignment is consistent with the report that a murine transmembrane FGFR1–alkaline phosphatase fusion protein can be cleaved in vitro by matrix metalloprotease-2 at an identical site (valine–methionine), just eight amino acids from the transmembrane domain [23].

4. Discussion

Since the initial identification of the soluble FGFRs in blood, efforts to predict their biological activities have been hampered by the incomplete chemical characterization of these proteins within the second half of the third Ig-like domain, where alternative splicing leads to receptor variants with different ligand binding properties. We have now mapped the amino acid sequence of the soluble FGFRs in this important region and show that the 55–60 kDa soluble FGFRs consist of two Ig-like domain isoforms of FGFR1(IIIa) and FGFR1(IIIc). The 85 kDa soluble FGFRs consist of the three Ig-like domain isoform of FGFR1(IIIc). The identification of a carboxyl-terminal peptide from FGFR1(IIIb), which is cleaved from the transmembrane receptor at a valine–methionine bond [23], suggests that the two and three Ig-like domain isoforms of soluble FGFR1(IIIb) are also present in blood.

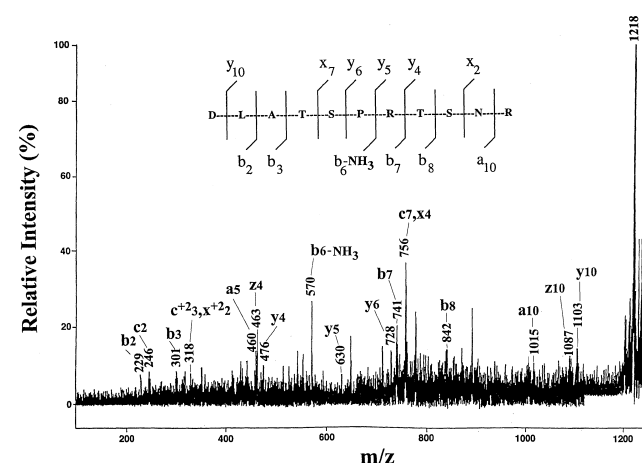Our results indicate that soluble FGFRs are generated from

Fig. 4. MALDI-PSD mass spectrum of the tryptic peptide D[250–260]R from the secreted FGFR(IIIa). The metastable ions resulting from the breakdown of the tryptic peptide 1217.6. The inset shows the expected sequence-specific fragment ions that were found in the spectrum. The fragmentation pattern corresponds to the a,b,c and x,y,z series cleavage sites. If the charge on the fragment ion remained on the N-terminus, the b series fragments (lower) are indicated. If the charge of the fragment ion remained on the C-terminus, the y series fragments (upper) are indicated. The peptide sequence ions are assigned using the nomenclature proposed by Biemann [22]. The additional peaks in the spectrum consist of ions that were likely generated from other peptides that were within the timed-ion selection window used to analyze the peptide of interest.

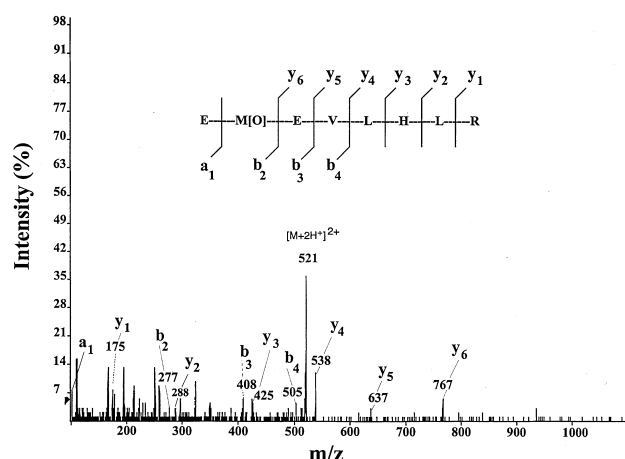[1] Trypsin does not cleave an arginine or lysine followed by a proline.

Fig. 5. NanoESI-MS/MS spectrum of the tryptic peptide E[211–218]R from a cleaved extracellular domain of FGFR1(IIIc). The fragment ion spectrum of the tryptic peptide MH^+ 1042.53 (the doubly charged peptide is $MH_2^{2+} = 521.2$). The inset shows the expected sequence-specific fragment ions that were found in the spectrum. 83% of the major peaks were identified. Most of the unlabeled peaks correspond to internal fragments.

the transmembrane FGFRs, FGFR1(IIIb) and FGFR1(IIIc), by proteolytic cleavage at the cell surface. Proteolytic processing of an extracellular domain at the cell surface is a common mechanism for releasing many soluble receptors, membrane bound growth factors and cell adhesion molecules and appears to be essential for normal physiologic growth, development and the response to stress [5,6].

In addition to cleaved soluble receptors, our results show that the secreted form of FGFR1(IIIa) circulates in blood. This result was conclusive and surprisingly unexpected, primarily because many soluble receptors that have been identified in vivo are produced by proteolytic cleavage at the cell surface and not by the secretion of the products of alternatively spliced mRNA transcripts [2,3]. However, tryptic fragments from the unique region of FGFR1(IIIa) were found by MS in three separate samples of purified material from calf serum and the assignment was confirmed using PSD, which gave an unequivocal fragmentation pattern of a tryptic peptide (DLATSPRTSNR) within the secreted FGFR. Thus, we conclude that both a secreted FGFR and multiple proteolytically cleaved FGFRs are present in calf serum. The secretion of a product of an alternatively spliced transcript and the proteolytic cleavage of full-length receptors are both mechanisms used to generate the circulating FGFRs. The relative contribution of each of these processes in vivo remains to be determined.

While the biological relevance of the soluble FGFRs is still unknown, it is intriguing to consider the possibility that the soluble FGFRs regulate the biological activities of the FGFs during growth and development. Using a semi-quantitative immunoassay with fresh human plasma, we have detected levels of the two and three Ig-like domain soluble FGFR isoforms at more than 500 ng/ml each (unpublished data). Such high circulating levels suggest that the soluble receptors could play an important regulatory role, even if their affinity for the FGFs is less than the affinities of the transmembrane FGFRs, as reported for a variety of recombinant forms of the soluble FGFRs [17,21,24]. Knowing the relative concentra-

tions of each of the five different soluble FGFR isoforms in blood, their affinities and ligand binding properties will give additional insight into their biological relevance.

The potential importance of these proteins as regulators of the FGF family members during growth and development is further emphasized by the phenotype of transgenic mice that overexpress a secreted form of FGFR2(IIIb) [25]. These non-viable mice have multiple defects that occur during early organogenesis. Most of the developmental abnormalities are consistent with an inhibition of FGFR signaling, indicating that the soluble receptor transgene functions as a dominant negative mutant and competes effectively with the full-length receptor for FGF binding. However, quite unexpectedly, the phenotype also shows craniofacial and skeletal abnormalities, which have also occurred with FGFR mutations that cause constitutive activation of the transmembrane receptor. In the future, it will be interesting to examine these effects in more detail and to determine how the soluble FGFRs regulate the biological activity of the FGFs in a variety of developmental and pathologic conditions.

References

[1] Rose-John, S. and Heinrich, P.C. (1994) J. Biochem. 300, 281–290.
[2] Mullberg, J., Althoff, K., Jostock, T. and Rose-John, S. (2000) Eur. Cytokine Netw. 11, 27–38.
[3] Werb, Z. and Yan, Y. (1998) Science 282, 1279–1280.
[4] Hooper, N.M., Karran, e.H. and Turner, A.J. (1997) Biochem. J. 321, 265–279.
[5] Tajima, Y., Moore, M.A.S., Soares, V., Ono, M.H.K. and Besmer, P. (1998) Proc. Natl. Acad. Sci. USA 95, 11903–11908.
[6] Peschon, J.J. et al. (1998) Science 282, 281–284.
[7] Hanneken, A.M., Ying, W., Ling, N. and Baird, A. (1994) Proc. Natl. Acad. Sci. USA 91, 9170–9174.
[8] Hanneken, A., Frautschy, S., Galasko, D. and Baird, A. (1995) NeuroReports 6, 886–888.
[9] Hanneken, A. and Baird, A. (1995) Invest. Ophthalmol. Vis. Sci. 36, 1192–1196.
[10] Hanneken, A., Maher, P. and Baird, A. (1994) J. Cell. Biol. 128, 1221–1228.
[11] Johnson, D.E. and Wiliams, L.T. (1993) Adv. Cancer Res. 60, 1–41.
[12] Dionne, C.A. et al. (1990) EMBO J. 9, 2685–2692.
[13] Johnson, D.E., Lee, P.L., Lu, J. and Williams, L.T. (1990) Mol. Cell. Biol. 10, 4728–4736.
[14] Johnson, D.E., Lu, J., Chen, H., Werner, S. and Williams, L.T. (1991) Mol. Cell. Biol. 11, 4627–4634.
[15] Keegan, K., Johnson, D.E., Williams, L.T. and Hayman, M.J. (1991) Proc. Natl. Acad. Sci. USA 88, 1095–1099.
[16] Partanen, J., Mäkelä, T.P., Eerola, E., Korhonen, J., Hirvonen, H., Claesson-Welsh, L. and Alitalo, K. (1991) EMBO J. 10, 1347–1354.
[17] Duan, D.R., Werner, S. and Williams, L.T. (1992) J. Biol. Chem. 267, 16076–16080.
[18] Ornitz, D.M., Xu, J., Colvin, J.S., McEwen, D.G., MacArthur, C.A., Coulier, F., Gao, G. and Goldfarb, M. (1996) J. Biol. Chem. 271, 15292–15297.
[19] Isacchi, A., Statuto, M., Chiesa, R., Bergonzoni, L., Rusnati, M., Sarmientos, P., Ragnotti, G. and Presta, M. (1991) Proc. Natl. Acad. Sci. USA 88, 2628–2632.
[20] Presta, M., Moscatelli, D., Joseph-Silverstein, J. and Rifkin, D. (1986) Mol. Cell Biol. 6, 4060–4066.

[21] Kiefer, M.C., Baird, A., Nguyen, T., George-Nascimento, C., Mason, O.B., Boley, L.J., Valenzuela, P. and Barr, P.J. (1991) Growth Factors 5, 115–127.

[22] Biemann, K. (1990) Methods Enzymol. 193, 886–887.

[23] Levi, E., Fridman, R., Miao, H.-Q., Ma, Y.-C., Yayon, A. and Vlodavsky, I. (1996) Proc. Natl. Acad. Sci. USA 93, 7069–7074.

[24] Olwin, B.B. and Hauschka, S.D. (1989) J. Cell Biochem. 39, 443–454.

[25] Celli, G., LaRochelle, W.J., Mackem, S., Sharp, R. and Merlino, G. (1998) EMBO J. 17, 1642–1655.

[26] Beer, H.D., Vindevoghel, L., Gait, M.J., Rivest, J.M., Duan, D.R., Mason, I., Dickson, C. and Werner, S. (2000) J. Biol. Chem. 275, 16091–16097.